

## The Mid-1970s Climate Shift in the Pacific and the Relative Roles of Forced versus Inherent Decadal Variability

GERALD A. MEEHL AND AIXUE HU

*National Center for Atmospheric Research,\* Boulder, Colorado*

BENJAMIN D. SANTER

*Program for Climate Model Diagnosis and Intercomparison, Lawrence Livermore National Laboratory, Livermore, California*

(Manuscript received 31 March 2008, in final form 23 July 2008)

### ABSTRACT

A significant shift from cooler to warmer tropical Pacific sea surface temperatures (SSTs), part of a pattern of basinwide SST anomalies involved with a transition to the positive phase of the Interdecadal Pacific Oscillation (IPO), occurred in the mid-1970s with effects that extended globally. One view is that this change was entirely natural and was a product of internally generated decadal variability of the Pacific climate system. However, during the mid-1970s there was also a significant increase of global temperature and changes to a number of other quantities that have been associated with changes in external forcings, particularly increases of greenhouse gases from the burning of fossil fuels. Analysis of observations, an unforced control run from a global coupled climate model, and twentieth-century simulations with changes in external forcings show that the observed 1970s climate shift had a contribution from changes in external forcing superimposed on what was likely an inherent decadal fluctuation of the Pacific climate system. Thus, this inherent decadal variability associated with the IPO delayed until the 1970s what likely would have been a forced climate shift in the 1960s from a negative to positive phase of the IPO.

### 1. Introduction

The mid-1970s were marked by a significant shift of conditions in the Pacific basin. This change was characterized by a pattern of tropical sea surface temperature (SST) anomalies and SST anomalies along the west coast of North America that went from cooler to warmer over the period of several years, while SSTs in the northwest and southwest Pacific cooled (Trenberth and Hurrell 1994). Such a shift is defined as a marked change in the pattern of base state SSTs that occurs at time scales longer than interannual. This pattern (shown later in Fig. 2c) has been associated with multidecadal variability in the Pacific that appears to be distinct from

El Niño interannual variability (Zhang et al. 1997). It has been shown that such a slowly varying pattern of SST anomalies, called the Interdecadal Pacific Oscillation (IPO) for the basinwide pattern (Power et al. 1999) or the Pacific decadal oscillation (PDO) for the North Pacific part of the pattern (Mantua et al. 1997), is associated with long-term fluctuations of Australian rainfall (Power et al. 1999; Arblaster et al. 2002) and a number of ecosystem impacts in the North Pacific (Mantua et al. 1997). Though there is the view that this pattern is not a deterministic mode of variability but rather amplitude modulation of El Niño events (e.g., Jin 2001), it has also been argued that there are distinct processes that form a mechanism to produce these slowly varying SSTs anomalies with some characteristics of a slow-motion delayed action oscillator (White et al. 2003). The details of the mechanism appear to rely on dynamically coupled tropical–midlatitude air–sea interactions that depend on the transit time of wind-forced ocean Rossby waves near 20°N and 20°S (Meehl and Hu 2006). These set the time scale for the multidecadal variability in the global coupled climate model—the

---

\* The National Center for Atmospheric Research is sponsored by the National Science Foundation.

---

*Corresponding author address:* Gerald A. Meehl, National Center for Atmospheric Research, P.O. Box 3000, Boulder, CO 80307.  
E-mail: meehl@ncar.ucar.edu

Parallel Climate Model (PCM) in that study. The PCM is the model analyzed in the present paper as described below.

The simulated response of the tropical Pacific Ocean to increasing greenhouse gases (GHGs) has some elements of a positive IPO pattern in terms of warming of tropical Pacific SSTs, as was first noted by Meehl and Washington (1996). This result has been substantiated by a majority of the recent generation of global coupled models, which show such a response to increasing GHGs (Meehl et al. 2007). Since GHGs were increasing throughout the twentieth century, with Pacific Ocean SSTs possibly responding with a pattern not unlike a positive IPO, there is thus the possibility that the mid-1970s shift to a more positive IPO state could have had an anthropogenic contribution.

The purpose of this paper is to address whether the mid-1970s climate shift was a natural product of inherent multidecadal climate variability, whether it was caused by increases of GHGs, or whether it was some combination of the two. We will rely on twentieth-century simulations from a global coupled climate model with a combination of anthropogenic and natural forcings, and simulations with anthropogenic forcings only and natural forcings only. An unforced control run will be analyzed to estimate the inherent multidecadal variability of the earth's climate system in the absence of changes in external forcings.

## 2. Model, observed data, and analysis framework

We use a fully coupled global climate model, the National Center for Atmospheric Research/Department of Energy Parallel Climate Model, which has been run in a number of twentieth-century experiments with both single forcings and various combinations of natural and anthropogenic forcings that all end in 1999 when the scenario twenty-first-century experiments were begun (Meehl et al. 2004). The resolution of the atmosphere is T42, or roughly  $2.8^\circ \times 2.8^\circ$ , with 18 levels in the vertical. Resolution in the ocean is roughly  $2\frac{2}{3}^\circ$  degree down to  $1\frac{1}{2}^\circ$  degree in the equatorial tropics, with 32 levels. The land surface model and a dynamic and thermodynamic sea ice formulation are fully described by Washington et al. (2000). No flux adjustments are used in the model. For the 1360-yr-long control integration, surface air temperatures show a small global-mean cooling trend of roughly 0.03 K per century. Here, we analyze a 300-yr period of the control integration. We use the same 300-yr period from the control run that was used in Meehl and Hu (2006) for consistency between the present study and that one. Analysis of longer or shorter periods does not affect the results since the dominant

multidecadal pattern from the control run is robust as noted below. Additionally, though this paper addresses multidecadal variability, it is worth noting that the ENSO component of interannual climate variability is in reasonable agreement with observations (Meehl et al. 2001).

The PCM produces inherent multidecadal variability with an IPO pattern in the Pacific. Meehl and Hu (2006) found that this pattern was associated with megadroughts in the southwest United States and South Asia—and (as noted above) identified a physical mechanism for this variability.

Compared to other models, the PCM is on the lower end of the climate sensitivity range, with an equilibrium climate sensitivity to a doubling of  $\text{CO}_2$  of  $2.1^\circ\text{C}$ , and a transient climate response (TCR, defined as the temperature change at the time of  $\text{CO}_2$  doubling in a 1% per year  $\text{CO}_2$  increase experiment) of  $1.3^\circ\text{C}$  (Meehl et al. 2004).

The observed SST dataset that we use is the Hadley Centre Sea Ice and Sea Surface Temperature dataset (HadISST1) produced by the Hadley Centre for the period 1890–2006 (Rayner et al. 2003). This is an improved and updated version of the previous Global Sea Ice and Sea Surface Temperature dataset (GISST) product. The HadISST data are reconstructed from observations by an EOF-based technique called reduced space optimal interpolation (RSOI) which is more reliable than simple EOF projection used in the previous GISST product. RSOI is applied as part of a two-step process. First the global pattern of long-term change is reconstructed, and then the residual interannual variability is reconstructed. In situ SST observations are then blended into the reconstructions to reintroduce local SST variance not represented in the larger-scale RSOI.

The HadISST1 dataset is one of a number of SST products used for climate studies, and all have their own unique characteristics and problems (e.g., Hurrell and Trenberth 1999; Folland et al. 2001). Some regional differences in Pacific SST trends in two products [HadISST1 and the NOAA Extended Reconstructed SST (ERSST)] were highlighted recently by Vecchi et al. (2008). Though the issues with the details of regional variability and trends must remain a caveat that accompanies any analysis of reconstructed SST data, the mid-1970s climate shift appears to be robust and was a notable feature observed not only in SSTs but in other related features in the Pacific (e.g., Mantua et al. 1997).

We compute EOFs of the nondetrended data [throughout the paper, we use the covariance matrix to compute the EOFs, thus facilitating comparisons of the magnitude of variability of the principal component (PC) time series],

and compare those with EOFs from 1) the unforced model control run, 2) a four-member ensemble average of twentieth-century simulations with a combination of natural and anthropogenic forcings (“all forcings”), and 3) a four-member ensemble average with natural forcings alone and a four-member ensemble average with anthropogenic forcings only. The difficulty of inferring “inherent” multidecadal variability from the observations is that it is impossible to achieve an unambiguous separation of the internally generated variability from the response to time-varying external forcings (Santer et al. 2006). Therefore, any set of EOFs estimated from the observations will be some combination of inherent variability and forced response. Model control runs, however, provide us with estimates of “pure” unforced variability. In the following, we rely on such simulations to deconstruct the climate variability in the Pacific and help to address the nature of the mid-1970s climate shift.

Another issue that arises in attempting to detect an unforced, decadal varying SST pattern in a forced twentieth century simulation is that the pattern associated with the mode of natural variability is fluctuating over time. In contrast, certain detection/attribution methods assume that the pattern of the searched-for “fingerprint” (the climate response to external forcing) is basically invariant, with the amplitude of the fingerprint increasing as the external forcing increases over time. Such methods seek to determine whether there is a significant, time-increasing expression of the fingerprint in observations (e.g., Santer et al. 1995). They are less appropriate for the present problem, which involves estimating the contribution of a quasiperiodic pattern to the mid-1970s shift.

Our approach, therefore, is to determine whether unforced variability alone (as manifest in a multi-hundred-year unforced PCM control run) could generate Pacific SST changes rivaling or exceeding those observed during the mid-1970s, or whether some combination of external forcing and internally generated variability provides the best explanation for the observed changes. Since the focus of this study is on low frequency variability, all model and observed data were low-pass filtered with a 13-yr cutoff, as in Meehl and Hu (2006). And, as also in that study, we are assuming that there are deterministic mechanisms that produce multidecadal variability in the Pacific that modulate the amplitude of ENSO events (e.g., White et al. 2003) as opposed to the opposite (e.g., Jin 2001) as discussed previously. Thus the low-pass filtering emphasizes the mechanisms operating at the multidecadal time scale.

It should be noted that, since different twentieth-century simulations were used as the initial states for the twenty-first century experiments, our all-forcings ex-

periments necessarily end in 1999 at the end of the twentieth century integrations. The twenty-first century experiments used initial states from anthropogenic forcings twentieth century experiments. Therefore, it is not possible to fill in early twenty-first century model data to append to the twentieth century simulations. For the purposes of our analyses here this is not a significant issue. However, since there was possibly a multidecadal shift to a negative IPO condition after the 1997–98 El Niño event (Lee and McPhaden 2008), we have included observations through 2006 in the EOF calculations. Owing to the 13-yr cutoff of the low-pass filter, the last nine years of the data drop off. Consequently, the plots of the PC time series of the observed low-pass filtered data end at the year 1997. This does not affect the interpretations of possible processes contributing to the mid-1970s climate shift.

### 3. Observed and inherent variability

Figure 1 shows the observed time series of globally averaged surface air temperature, which increases in the first half of the twentieth century, levels out from about the mid-1940s to the mid-1970s, and then transitions to rapidly increasing temperatures starting in the mid-1970s (Meehl et al. 2004). This mid-1970s change is not captured in the mean of the four-member PCM ensemble with natural forcings only, but is reproduced with the addition of anthropogenic forcings in the “all forcings” case (Fig. 1). Meehl et al. examine single forcing ensembles with this model and conclude that most of the warming prior to 1940 was natural (largely due to increasing solar forcing), and after the mid-1970s it was mostly anthropogenic. Thus, since anthropogenic forcing made a substantial contribution to this particular climate change in the mid-1970s (in terms of globally averaged surface air temperatures), perhaps there was some contribution of anthropogenic forcing to the climate shift in the Pacific that occurred at that same time.

Turning our attention to the Pacific basin, Fig. 2 shows the first two EOFs of the nondetrended low-pass filtered observed SST data for the period from 1890 to 2006 (the low-pass filter cuts off the first and last nine years as noted above). The first EOF accounts for 47.4% of the variance and has mostly a basinwide warming with some negative values in the equatorial eastern Pacific. Linear trends of unfiltered SSTs show most of the eastern equatorial Pacific cooling occurred in the first half of the twentieth century (not shown). Consequently, the PC time series has increasing values from the early 1900s to the 1940s indicating warming over most of the basin and some areas of equatorial eastern Pacific cooling, with low amplitude oscillations

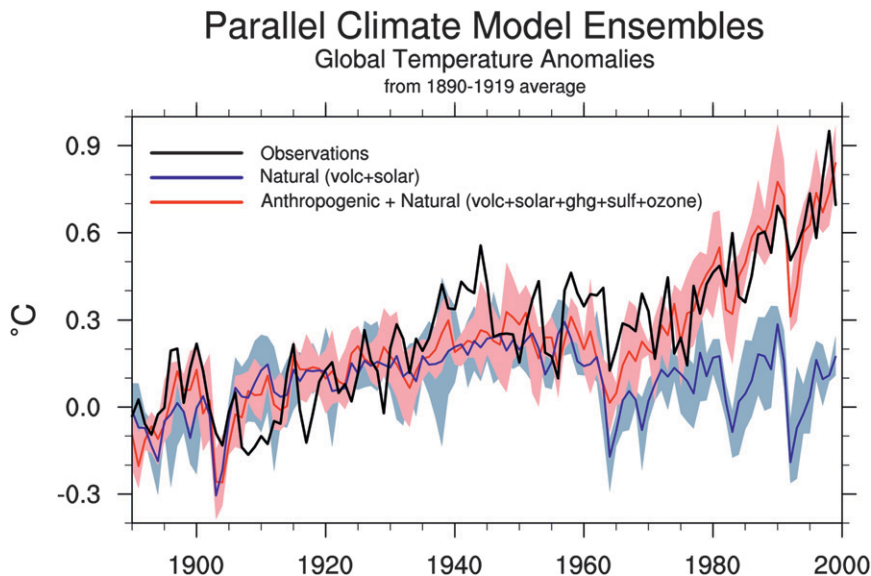


FIG. 1. Four-member ensemble mean (red line) and ensemble member range (pink shading) for globally averaged annual surface air temperature anomalies ( $^{\circ}\text{C}$ ; anomalies are formed by subtracting the 1890–1919 mean for each run from its time series of annual values) for natural and anthropogenic forcings [(volcano + solar + GHG + sulfate + ozone)]; solid blue line is ensemble mean, and light blue shading is ensemble range for globally averaged temperature response to natural forcings only [(volcano + solar)]; black line is observations; (after Meehl et al. 2004).

thereafter. Note that the sign of an EOF is arbitrary, but here and elsewhere we interpret the EOF patterns depicted in the figures corresponding to positive values in the PC time series, and the opposite sign of the pattern with negative values in the PC time series.

The second EOF of observed Pacific SSTs (Fig. 2c), explaining 24.6% of the variance, is reminiscent of the “decadal” Pacific pattern described in other studies (e.g., Zhang et al. 1997; Power et al. 1999; Meehl and Hu 2006). As discussed in the introduction, the North Pacific part of this pattern has been referred to as the PDO (Mantua et al. 1997), while the Pacific basinwide multidecadal pattern of Zhang et al. (1997) has been called the IPO (Power et al. 1999). It has a broad area of positive values in the tropical Pacific and along the west coasts of North and South America, with opposite sign values in the northwest and southwest Pacific. Since our focus is on Pacific basinwide multidecadal variability, throughout this paper we will refer to the pattern in Fig. 2c as the “IPO,” and the phase when tropical Pacific values are positive as depicted in Fig. 2c as a “positive IPO” corresponding to positive values of the PC time series, with opposite signs for negative values of the PC time series. There is a sharp transition from negative to large positive values of the PC time series that occurred in less than five years in the mid-1970s (i.e., the pattern rapidly shifted from negative to positive IPO during the

mid-1970s). This is the climate shift we will attempt to diagnose in the present paper.

To test the stability and time evolution of these patterns, an EOF analysis of the observed SSTs from 1940 to 2006 shows the IPO pattern is EOF1, with 57.5% of the variance explained (not shown). This is because the mid-1970s shift becomes that major event of the second half of the twentieth century as indicated by the PC time series from that shorter period (not shown). An EOF analysis of an even shorter period from 1970 to 2006, clearly questionable to address low-pass filtered multidecadal variability with only 37 years of data, consequently shows a dominant EOF1 with 62.4% of explained variance with a pattern characterized by warming over most of the Pacific basin, reflecting the general warming trend over that time period.

The first EOF from the unforced model control run (Fig. 3a) is characterized by an IPO pattern similar in some respects to the observed IPO in Fig. 2c, with a pattern correlation of +0.63. This implies that PCM is capturing at least some aspects of an observed pattern of multidecadal SST variability. A spectral analysis of the PC time series in Fig. 3b reveals significant periods (compared to the red noise spectrum) of around 18, 25, and 50 yr (not shown). The EOF1 pattern from the model control run in Fig. 3 explains 36.1% of the variance. The second and third EOFs, explaining 14.4% and 8.5% of

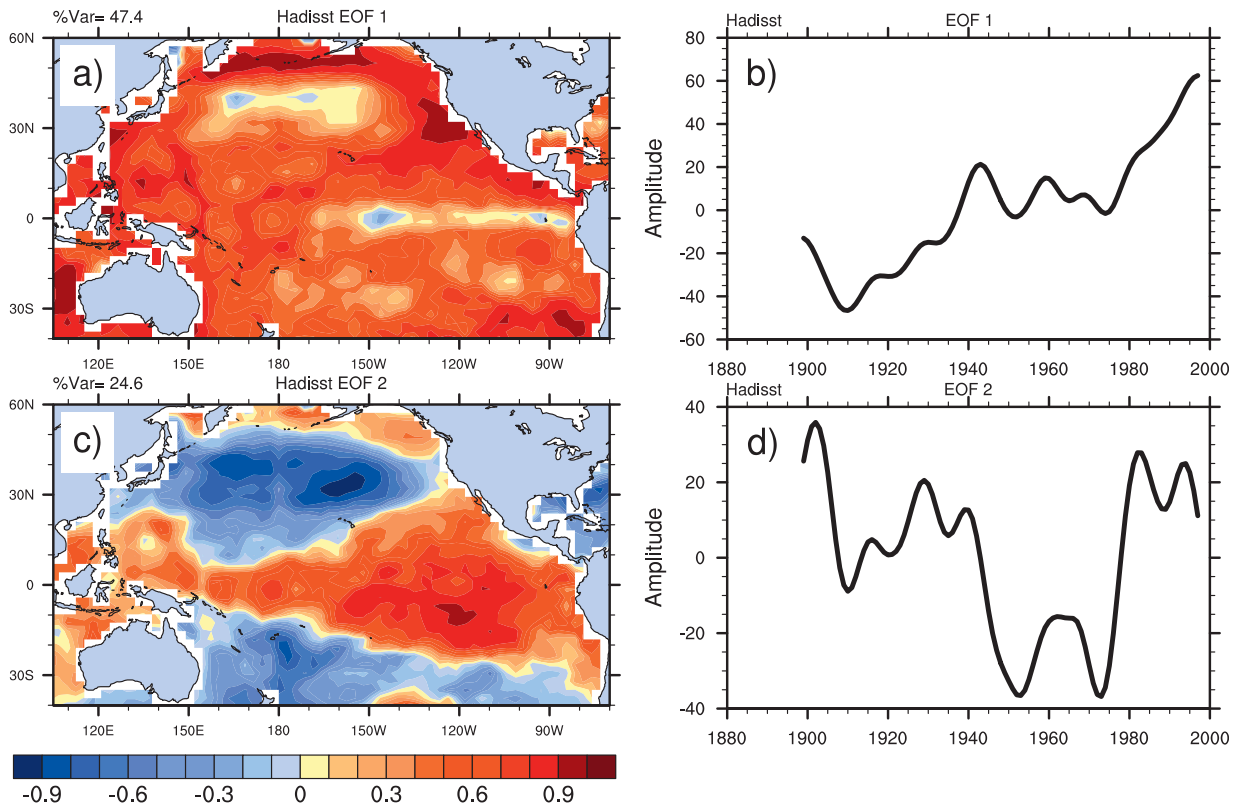


FIG. 2. The (a) first EOF and (c) second EOF of 13-yr low-pass-filtered nondetrended observed SSTs for the period 1890–2006; PC time series for the (b) first EOF and (d) second EOF.

the variance respectively, also are characterized by IPO-like patterns (not shown) indicating the dominance of this pattern in the unforced control run. Splitting the record into 100-yr segments and performing the EOF analysis on those subperiods shows similar results to the longer 300-yr period with comparable patterns and explained variances for the first three EOFs. An even longer period from the control run shows similar results as well, indicating the IPO pattern is a robust feature of inherent multidecadal variability in this model. As noted earlier, we use the same 300-yr period from the control run here that was used in Meehl and Hu (2006) for consistency between the present study and that one.

Since the observed SST changes are a mix of forced and unforced variability, there is still the issue of the relative contributions that these changes receive from external forcing and internal variability of the climate system. Note that all pattern correlations in this paper are uncentered, that is, the spatial means are included. Though a less stringent test of pattern similarity, uncentered pattern correlations are more relevant for interpreting the relative contributions when we project filtered SST changes onto forced and unforced patterns of SST variability below.

Next, we consider the relationship between decadal time-scale SST variability in the Pacific and variability in global-mean surface air temperature. If there is a direct connection between IPO changes in the Pacific and globally averaged temperatures it may be possible to infer relative contributions of forcing and natural variability from globally averaged temperatures to the IPO. However, for the observations, a similar problem to the one outlined above applies; that is, it is unclear how much of the IPO “decadal” pattern (Fig. 2c) is forced (and thus could demonstrate a connection to the forced response of the ensemble-mean model simulations of globally averaged surface air temperature in Fig. 1) and how much could be inherent variability and, thus, part of the “noise” that is removed by ensemble averaging the model simulations.

To identify a linkage between globally averaged surface air temperature and the IPO, we correlate the PC time series of the model IPO (Fig. 3b) with the corresponding time series of globally averaged surface air temperature from the control run. This correlation is +0.42, which is significant at greater than the 1% level after removing autocorrelation effects from each low-pass filtered time series as in Leith (1973). Thus in PCM,

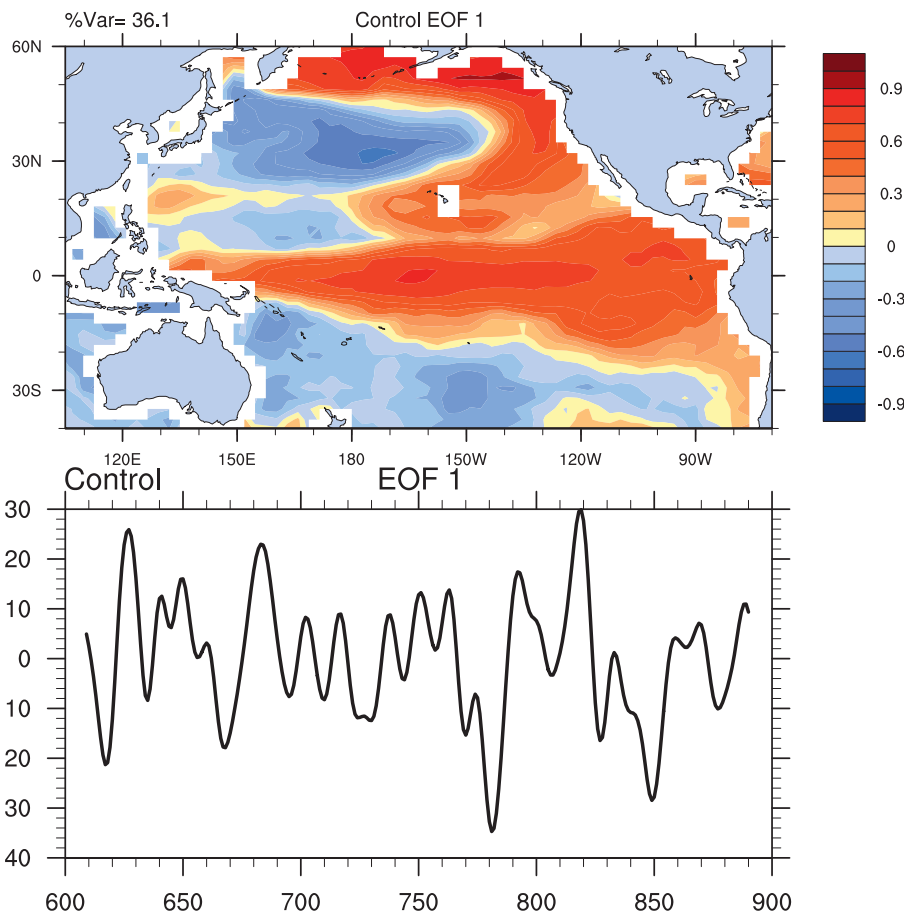


FIG. 3. (a) The first EOF of 13-yr low-pass-filtered SSTs from a 300-yr period of the unforced model control run and (b) PC time series for first EOF.

the inherent pattern of multidecadal variability in the Pacific is significantly related to globally averaged temperature, with a warmer tropical Pacific associated with higher globally averaged temperatures, and vice versa for a cooler tropical Pacific. However, the conclusion from Fig. 1 was that most of the globally averaged temperature trend after the 1970s was a forced response. Since there is a high correlation between globally averaged temperature and the IPO in the model, the inherent pattern of decadal SST variability in the Pacific, the IPO, also must be related in some way to the forced response, which we address next.

#### 4. Forced response compared to the observations

Figure 4 shows the first and second EOFs from the ensemble mean of the all-forcings simulations from the model. The first EOF displays warming almost everywhere except the northwest Pacific, with greatest warming in the tropics (Fig. 4a). This is similar to the anthropogenic forced response pattern from the model

(Fig. 5a) with a pattern correlation of  $+0.92$ . The PC time series from the first EOF (Fig. 4b) increases throughout the twentieth century, with the largest rate of increase after the mid-1960s. The second EOF from the ensemble mean all-forcings model simulations (Fig. 4c) also has some similarities to the IPO in the unforced EOF1 pattern in Fig. 3a (pattern correlation of  $+0.45$ ), though the pattern correlation with EOF2 from the observations is only  $+0.03$ .

As was the case for the EOF1 PC time series in Fig. 4b, a striking aspect of the second half of the twentieth century in the EOF2 PC time series (Fig. 4d) is a transition from negative to positive values that starts in the mid-1960s. Recall that these are PC time series estimated from *ensemble-mean* SST changes in the PCM all-forcings experiment and that each of the four realizations of this experiment has a different manifestation of climate “noise” (internally generated natural variability) superimposed on the underlying “signal” (the response to the time-varying external forcings). Ensemble averaging damps this noise, and provides a

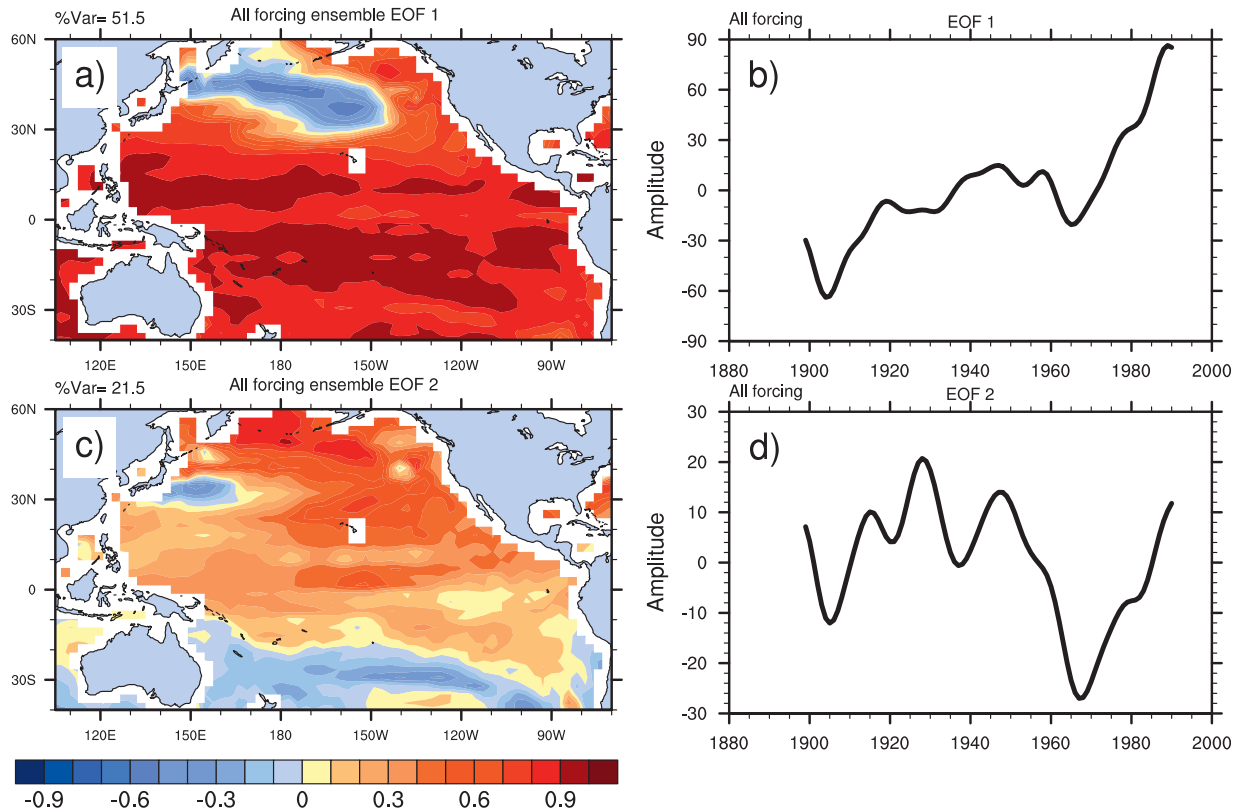


FIG. 4. The (a) first EOF and (c) second EOF of 13-yr low-pass-filtered SSTs for the ensemble-mean all-forcings model experiment for the period 1870–2000; PC time series for (b) first EOF and (d) second EOF.

better estimate of the true response to the imposed forcing changes. So if the “real world” mid-1970s climate shift was due to climate noise (internally generated inherent climate variability) alone, we would not expect the *ensemble mean* of the PCM all-forcings experiment to replicate this change. The fact that both the EOF1 PC time series and EOF2 PC time series of the all-forcings experiment show pronounced increases close to the time of the observed mid-1970 climate shift implies that external forcing may, indeed, have contributed to the shift in the observations.

As noted above, the conclusion derived from Fig. 1 is that anthropogenic forcings were influential in producing most of the warming in the latter part of the century, while natural forcings, particularly an increase of solar forcing, produced most of the warming in the first part of the twentieth century (Stott et al. 2000; Meehl et al. 2004; Knutson et al. 2006). The latter result is supported by the PCM response to increasing solar forcing during the first half of the twentieth century, with warming over most of the Pacific except for cooling in the equatorial eastern Pacific (Meehl et al. 2003, 2008). The observations also show elements of this pattern for EOF1 (Fig. 2a) with a positive trend in

this pattern during the first half of the twentieth century (Fig. 2b).

To verify that the model replicates key features of the observations, the leading EOF of the ensemble mean of twentieth century simulations with just anthropogenic forcings (Fig. 5a) shows warming over most of the basin, with a PC time series that has small increases in the first half of the century until a more steep increase starts in the 1960s (Fig. 5b). As noted earlier, this is very similar (pattern correlation of +0.92) to the first EOF from the all-forcings ensemble mean (Fig. 4a), thus indicating that much of the response seen in the all-forcings experiment in the latter part of the twentieth century (Fig. 4b) is due to anthropogenic forcing (Fig. 5b).

Alternately, Fig. 5c shows EOF1 from an ensemble mean of model simulations of twentieth century climate with only natural forcings (solar and volcanoes) included. Consistent with the Meehl et al. (2003) result, Fig. 5c shows mostly positive values, with negative values only in the eastern equatorial Pacific, and a large positive trend in this pattern in the PC time series in the first half of the twentieth century (Fig. 5d). This is consistent with the trend in observed SSTs for the first half of the twentieth century that shows warming

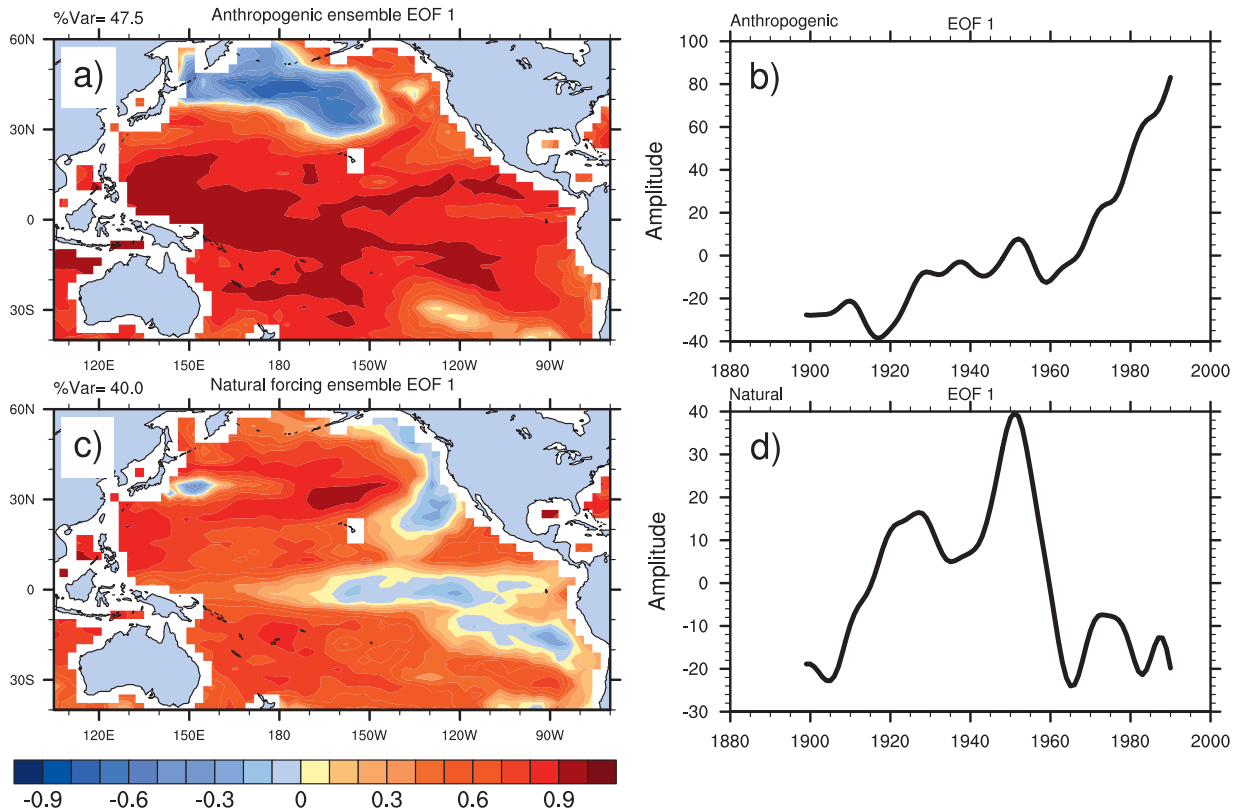


FIG. 5. The first EOF of 13-yr low-pass-filtered SSTs for (a) the ensemble-mean anthropogenic forcings experiment for the period 1870–2000 and (c) the ensemble-mean natural forcings experiment; PC time series for (b) the first EOF and (d) the ensemble-mean natural forcings experiment.

almost everywhere except cooling in the equatorial eastern Pacific (not shown).

Figure 2a from the observations and Fig. 5c from the natural forcings experiment both show warming over most of the basin and negative values in the equatorial eastern Pacific. Though the natural forcings ensemble also includes volcanoes, Meehl et al. (2004) showed in single forcing experiments that most of the increase in temperatures in the first part of the twentieth century is related to increases in solar forcing, and a cooler eastern equatorial Pacific is the signature of increasing solar forcing in the first half of the twentieth century (Meehl et al. 2003). The PC time series from the observations (Fig. 2b) and model natural forcings experiment (Fig. 5d) both show large positive trends for the first half of the twentieth century, indicating warming over most of the basin with small cooling in the equatorial eastern Pacific. Meanwhile the anthropogenic-only EOF1 pattern (Fig. 5a) is more comparable to the EOF2 pattern from the observations (Fig. 2c) in that both show a warmer tropical Pacific. However, the overall pattern correlation is not significant and the PC time series from these two EOFs are quite different. From the model

anthropogenic experiment there is a transition in the 1960s (Fig. 5b), while for the observations there are more decadal-time-scale fluctuations (Fig. 2d). The fact that the inherent pattern of multidecadal variability in the unforced control run (Fig. 3a) shows a similar pattern to the observed EOF2 (Fig. 2c) implies that the contributions from inherent multidecadal variability are mixed in with the response to anthropogenic forcings. Therefore, we are faced with the challenge of having to disentangle similar patterns arising from inherent variability and forced response.

### 5. Understanding the 1970s climate shift

So far we have analyzed multimember ensemble-mean model simulations of twentieth century climate with various combinations of natural and anthropogenic forcings. By looking at ensemble averaged model data, the internally generated inherent variability is damped, assuming the decadal variability is occurring randomly in the different model ensemble members. Therefore, such inherent variability is mostly removed in an ensemble average. However, as noted above, the real twentieth

century climate probably had a combination of inherent variability and forced response. We have identified elements of a common pattern present in both forced and unforced simulations, the IPO pattern, first identified in observations (e.g., Zhang et al. 1997) and defined by Power et al. (1999). But since elements of this pattern appear in both forced and unforced simulations, interpretation of the 1970s climate shift that involved this pattern becomes more difficult. Additionally, ensemble averages from a model have clear limitations when trying to apply them to interpreting the single realization from the observations.

Therefore, since the observed twentieth century climate is a single realization with a combination of inherent variability and forced response, the approach that we take is to find an example of a single member from the climate model all-forcings ensemble with somewhat comparable variability as an analog. This should include a transition that started in the 1960s and another that occurred a bit later. Since we have identified the 1960s as a time when the effects of anthropogenic forcing could be seen in the ensemble means and the 1970s as a time when a shift occurred in the observations, we will attempt to infer relative anthropogenic and inherent contributions to these shifts in the single ensemble member with comparable changes and then apply this technique to the single realization of the observations.

Figure 6a shows the first EOF from the example chosen from the all-forcings simulations, with the PC time series in Fig. 6b as the dark solid line. There is a high degree of correspondence between the observed and model simulated EOF patterns in Figs. 6a and 2c (pattern correlation of +0.70) with both showing a dominant positive IPO pattern. Note that EOF1 from this particular ensemble member (Fig. 6a) is less like the corresponding EOFs from the all-forcings ensemble mean (Fig. 4, no significant pattern correlation) and more like the inherent pattern of variability in the unforced control run (Fig. 3a, pattern correlation of +0.77). This implies that there could be a large contribution from inherent multidecadal variability in this particular ensemble member compared to the forced response in the ensemble mean and that some insight could be obtained from this ensemble member to help interpret the observed mid-1970s shift.

Next, we project the EOF1 SST pattern from the unforced control run (Fig. 3a) onto the low-pass filtered SST data from the single ensemble member in Fig. 6a and produce a time series of the pattern correlations in Fig. 6b (dotted line). Then we do a similar calculation using the forced response patterns (EOF1 and EOF2 in Figs. 4a and 4c, respectively) from the all-forcings en-

semble mean (all-forcings EOF1 pattern correlation is dash-dot; all-forcings EOF2 pattern correlation is dashed). The pattern correlations with the control run EOF should show the time evolution of the relative contribution from inherent variability, while the pattern correlations from the first two EOFs from the ensemble mean all-forcings experiment should indicate the time-evolving contribution from external forcing. The time series of pattern correlations from these calculations are plotted in Fig. 6b. We then compare the time evolution of these three time series with the EOF1 PC time series in Fig. 6b (dark solid line). Note that we do not correlate any of the pattern correlation time series with the EOF1 PC time series in Fig. 6b. Rather, the explained variance numbers below are the squares of the pattern correlations at different times in the individual time series.

This ensemble member was chosen for its EOF1 pattern that resembles the IPO and its consequent fluctuations of the IPO in the second half of the twentieth century. The EOF1 PC time series in Fig. 6b (dark solid line) shows what appears to be the beginning of a transition from a negative to positive IPO in the mid-1960s (going from negative values toward positive in the PC time series: thin vertical line drawn at 1965 for reference). That is interrupted by a return to negative values after 1975 (denoted by another thin vertical line for reference) and then a significant shift starting in about 1980 where the PC time series makes a rapid transition in less than five years from negative to positive values indicative of a shift to a positive IPO state (thin vertical line drawn for reference at 1980).

To help interpret this time evolution of the IPO pattern represented by the PC time series in this ensemble member, we compare the pattern correlation time series to the PC time series at various times. The pattern correlations from inherent multidecadal variability in the unforced control run indicate that the mid-1960s change (dotted line, pattern correlations of about +0.5) had a contribution from inherent variability that explained about 25% of the variance (here and elsewhere the square of the pattern correlation calculated from the original low-pass filtered SST data) and an additional 25% of the variance (pattern correlation of about +0.5) from forced variability involved with EOF2 from the all-forcing experiment (dashed line in Fig. 6b). The movement of the PC time series from negative to near-zero values in the mid-1970s had a significant inferred contribution from the forced EOF1 (dash-dot) with a pattern correlation of almost +0.5 in that time period for an explained variance of nearly 25%.

Since the first EOF from this single ensemble member could have both forced and inherent contributions to its pattern (and to EOFs other than the first, though they

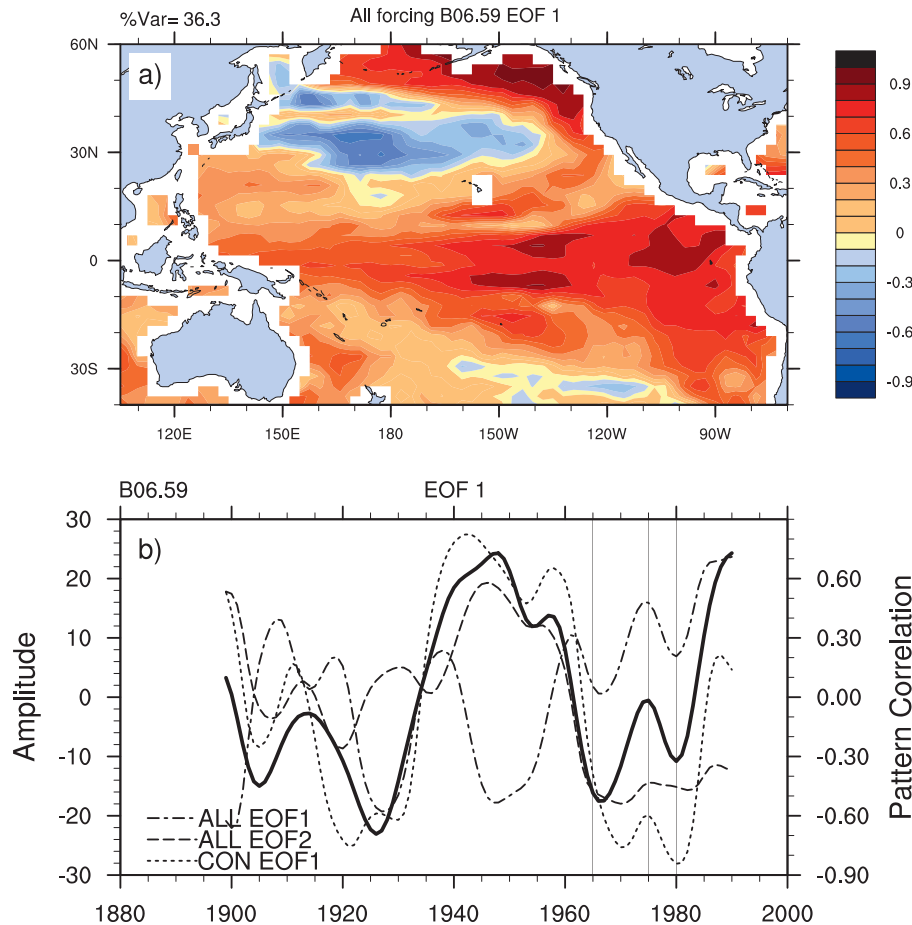


FIG. 6. (a) The first EOF from a single ensemble member from the low-pass-filtered SSTs in an all-forcings experiment; (b) PC time series from the single ensemble member (solid) and pattern correlations from projecting the first EOF from the control run (Fig. 3) onto the low-pass-filtered SST data from the single ensemble member (dotted) and similarly from projecting the first (dash-dot) and second (dashed) EOFs from the ensemble-mean all-forcings experiment (Figs. 4a and 4c, respectively) onto the low-pass-filtered SST data from the single ensemble member. The left axis labels refer to the amplitude of the PC time series (dark solid line), and the right axis labels are for the amplitude of the pattern correlations (dash-dot, dashed, and dotted lines). Thin vertical lines denote 1965, 1975, and 1980 as discussed in text.

explain only about 18% for the second and 16% for the third), the pattern correlation explained variance estimates can only be interpreted as indicative of possible relative contributions. But this calculation suggests that, during the 1960s in this ensemble member, there were nearly equal contributions from both forced and inherent variability. We infer that most of the change in the IPO as it went from negative to near-zero values in the mid-1970s was likely due to a forced response.

The early 1980s return to a more negative IPO in the PC time series was mostly due to inherent variability with pattern correlations from the control EOF1 in excess of  $-0.8$  at that time (dotted line), thus explaining over 70% of the pattern variance. The forced response

from the two ensemble mean all-forcings EOFs explain 20% of the pattern variance each for that same time period. As the PC time series recovers and transitions to positive values indicative of a positive IPO after the early 1980s, the contribution to the pattern from inherent variability (dotted line) also goes from negative to positive pattern correlations, and the forced EOF1 (dash-dot line) is the dominant contributor to the positive IPO, explaining nearly 50% of the pattern variance by 1990.

These results imply that the forced change that started to occur in the 1960s was delayed about 15 yr due to a very large inherent climate fluctuation that occurred in this ensemble member in the early 1980s. In this

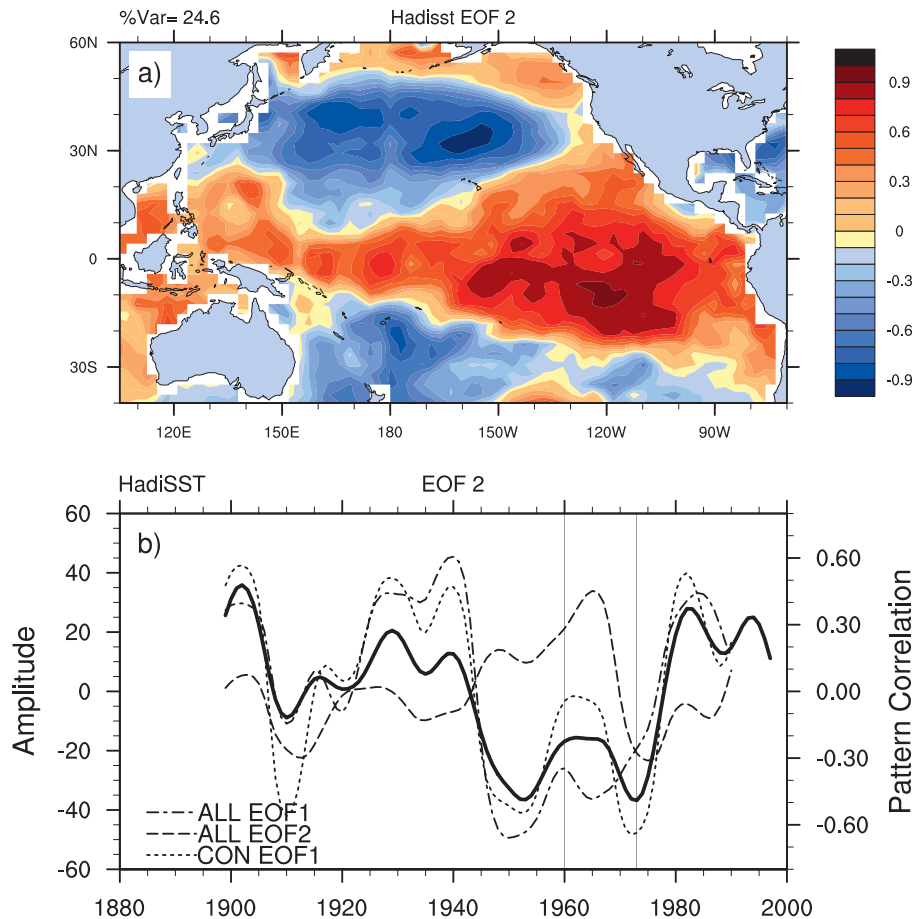


FIG. 7. (a) The second EOF from the low-pass-filtered SST observations (as in Fig. 2c); (b) PC time series from the second EOF from the observations (solid, as in Fig. 2d) and pattern correlations from projecting the first EOF from the control run (Fig. 3) onto the low-pass-filtered observed SST (dotted) and similarly from projecting the first (dash-dot) and second (dashed) EOFs from the ensemble-mean all-forcings experiment (Figs. 4a and 4c, respectively) onto the low-pass-filtered observed SST data. The left axis labels refer to the amplitude of the PC time series (dark solid line), and the right axis labels are for the amplitude of the pattern correlations (dash-dot, dashed, and dotted lines). Thin vertical lines denote 1960 and 1973 as discussed in text.

example, the Pacific climate system shifted into a strong positive IPO pattern when forcing and inherent variability acted in the same direction with positive pattern correlations.

We now apply this technique to the IPO pattern from observed EOF2 in Fig. 7a. We project the same model-generated EOFs as in Fig. 6 onto the low-pass filtered observed SSTs and compare the time series of the pattern correlations to the PC time series of EOF2 (dark solid line) in Fig. 7b.

During the 1960s, the forced EOF2 (dashed line) shows large positive pattern correlations of about +0.5, or 25% of the pattern variance that seemingly should have contributed to a more positive IPO pattern (Fig. 7b; thin vertical line is drawn at 1960 for reference). However, the values of the PC time series actually be-

come more negative (thus a more negative IPO) in the late 1960s and early 1970s (thin vertical line is drawn at 1973 for reference). There is a dominant contribution to a negative IPO from inherent variability inferred from the pattern correlations with the EOF1 model control run approaching  $-0.7$  or nearly 50% of the explained pattern variance in the early 1970s. Then there is the large shift in the PC time series from negative to positive values in the mid- to late 1970s. This occurred in conjunction with contributions to a positive IPO from positive pattern correlations of about +0.55 from inherent variability (reaching nearly 30% of the explained pattern variance) around 1980 and an additional positive contribution from the forced EOF1 (nearly 20% of the explained variance in the early 1980s). As in the example using one of the model ensemble members, it

appears that the combination of forced and inherent variability produced the observed shift from a negative to a positive IPO state by the early 1980s.

The inference for the observed Pacific climate system is that a shift from a negative IPO to positive IPO should have started occurring in the 1960s, but was likely delayed about 10 yr due to a large inherent climate fluctuation in the early 1970s that produced a return to negative IPO conditions followed by the turnaround in the EOF2 PC time series to a more positive IPO state (dark solid line in Fig. 7b). From this analysis we can speculate that, without the influence of inherent variability in the 1970s, a shift from negative to positive IPO would have occurred in the 1960s. When the shift did occur in the 1970s, it was large and dramatic, as both forced and unforced responses were working in the same direction at the same time to produce the transition to a positive IPO pattern.

The forced climate change that tried to start in the 1960s in the Pacific basin could be related to other changes around the globe at that time (Baines and Folland 2007). Addressing this wider issue is beyond the scope of the present paper.

## 6. Conclusions

We examine the 1970s climate shift, a time when the IPO pattern in Pacific SSTs transitioned from negative to positive in less than 5 yr, and address how much of it was natural and how much was forced. In an analysis of observations, EOF1 of low-pass filtered SST is characterized by a warming over almost the entire basin in the first half of the twentieth century except for cooling in the equatorial eastern Pacific. Model simulations with single forcings and a combination of natural forcings suggest that this early century response is mainly a reaction to increased solar forcing during this time period as shown in other studies. Later in the century, the observed EOF2 PC time series shows a large climate shift in the mid-1970s, with Pacific basin SSTs transitioning from a negative to positive IPO pattern.

The cause of this shift is made more ambiguous since model simulations show that a positive IPO pattern characterizes some aspects of the trend in the ensemble-mean response to anthropogenic forcing, as well as being the dominant mode of unforced inherent multi-decadal variability. Since the inherent IPO decadal pattern fluctuates with time, more conventional detection/attribution methodologies are not appropriate since they typically search for a pattern that grows with time. Therefore, we first infer relative contributions from inherent variability in comparison to the forced response pattern by projecting the inherent and forced patterns

separately on low-pass filtered SSTs from a single model ensemble member. This ensemble member is chosen as an example of a climate realization where Pacific SSTs are characterized by an EOF1 pattern that resembles the IPO pattern from observations, with a Pacific climate fluctuation in the 1960s and a subsequent shift to a positive IPO state by the end of the century. The small 1960s climate shift in this member has nearly equal inferred contributions from inherent and forced patterns, while a subsequent shift in the early 1980s occurs when inherent and forced variability act in concert to contribute to a rapid transition to a positive IPO pattern.

Next, we apply that same diagnostic to the observations to try and understand the possible contributions to the 1970s climate shift in the Pacific that was characterized by a notable transition from a negative to positive IPO pattern in only a few years. Separately projecting the forced and inherent patterns from the model onto the low-pass filtered SST observations, and comparing those pattern correlations to the time evolution of the PC time series, indicates a contribution to a potential climate shift in the 1960s due to anthropogenic forcing. However, a large inherent decadal fluctuation in the mid-1970s delayed the shift that would have otherwise occurred in the 1960s due to changes in forcing. The rapid transition in the 1970s was due to the combination of inherent variability and forced response, acting in the same direction at the same time, thus contributing to the shift to a positive IPO pattern.

*Acknowledgments.* Portions of this study were supported by the Office of Science (BER), U.S. Department of Energy, Cooperative Agreement DE-FC02-97ER62402, and the National Science Foundation.

## REFERENCES

- Arblaster, J. M., G. A. Meehl, and A. Moore, 2002: Interdecadal modulation of Australian rainfall. *Climate Dyn.*, **18**, 519–531.
- Baines, P. G., and C. K. Folland, 2007: Evidence for a rapid global climate shift across the late 1960s. *J. Climate*, **20**, 2721–2744.
- Folland, C. K., and Coauthors, 2001: Global temperature change and its uncertainties since 1861. *Geophys. Res. Lett.*, **28**, 2621–2624.
- Hurrell, J. W., and K. E. Trenberth, 1999: Global sea surface temperature analyses: Multiple problems and their implications for climate analysis, modeling, and reanalysis. *Bull. Amer. Meteor. Soc.*, **80**, 2661–2678.
- Jin, F.-F., 2001: Low-frequency modes of tropical ocean dynamics. *J. Climate*, **14**, 3874–3881.
- Knutson, T. R., and Coauthors, 2006: Assessment of twentieth-century regional surface temperature trends using the GFDL CM2 coupled models. *J. Climate*, **19**, 1624–1651.
- Lee, T., and M. J. McPhaden, 2008: Decadal phase change in large-scale sea level and winds in the Indo-Pacific region at the end

- of the 20th century. *Geophys. Res. Lett.*, **35**, L01605, doi:10.1029/2007GL032419.
- Leith, C. E., 1973: The standard error of time-average estimates of climatic means. *J. Appl. Meteor.*, **12**, 1066–1069.
- Mantua, N. J., S. R. Hare, Y. Zhang, J. M. Wallace, and R. C. Francis, 1997: A Pacific interdecadal oscillation with impacts on salmon production. *Bull. Amer. Meteor. Soc.*, **78**, 1069–1079.
- Meehl, G. A., and W. M. Washington, 1996: El Niño-like climate change in a model with increased atmospheric CO<sub>2</sub> concentrations. *Nature*, **382**, 56–60.
- , and A. Hu, 2006: Megadroughts in the Indian monsoon region and southwest North America and a mechanism for associated multi-decadal Pacific sea surface temperature anomalies. *J. Climate*, **19**, 1605–1623.
- , P. Gent, J. M. Arblaster, B. Otto-Bliesner, E. Brady, and A. Craig, 2001: Factors that affect amplitude of El Niño in global coupled climate models. *Climate Dyn.*, **17**, 515–526.
- , W. M. Washington, T. M. L. Wigley, J. M. Arblaster, and A. Dai, 2003: Solar and greenhouse gas forcing and climate response in the twentieth-century. *J. Climate*, **16**, 426–444.
- , —, C. Ammann, J. M. Arblaster, T. M. L. Wigley, and C. Tebaldi, 2004: Combinations of natural and anthropogenic forcings and twentieth-century climate. *J. Climate*, **17**, 3721–3727.
- , and Coauthors, 2007: Global climate projections. *Climate Change 2007: The Physical Science Basis*, S. Solomon et al., Eds., Cambridge University Press, 747–845.
- , J. M. Arblaster, G. Branstator, and H. Van Loon, 2008: A coupled air–sea response mechanism to solar forcing in the Pacific region. *J. Climate*, **21**, 2883–2897.
- Power, S., T. Casey, C. Folland, A. Colman, and V. Mehta, 1999: Interdecadal modulation of the impact of ENSO on Australia. *Climate Dyn.*, **15**, 319–324.
- Rayner, N., D. Parker, E. Horton, C. Folland, L. Alexander, D. Rowell, E. Kent, and A. Kaplan, 2003: Global analyses of sea surface temperature, sea ice, and night marine air temperature since the late nineteenth century. *J. Geophys. Res.*, **108**, 4407, doi:10.1029/2002JD002670.
- Santer, B. D., U. Mikolajewicz, W. Brüggemann, U. Cubasch, K. Hasselmann, H. Höck, E. Maier-Reimer, and T. M. L. Wigley, 1995: Ocean variability and its influence on the detectability of greenhouse warming signals. *J. Geophys. Res.*, **100**, 10 693–10 725.
- , and Coauthors, 2006: Causes of ocean surface temperature changes in Atlantic and Pacific hurricane formation regions. *Proc. Natl. Acad. Sci. USA*, **103**, 13 905–13 910.
- Stott, P. A., S. F. B. Tett, G. S. Jones, M. R. Allen, J. F. B. Mitchell, and G. J. Jenkins, 2000: External control of 20th century temperature by natural and anthropogenic forcings. *Science*, **290**, 2133–2137.
- Trenberth, K. E., and J. W. Hurrell, 1994: Decadal atmosphere–ocean variations in the Pacific. *Climate Dyn.*, **9**, 303–319.
- Vecchi, G. A., A. Clement, and B. J. Soden, 2008: Examining the tropical Pacific’s response to global warming. *Eos, Trans. Amer. Geophys. Union*, **89**, 81–83.
- Washington, W. M., and Coauthors, 2000: Parallel climate model (PCM) control and transient simulations. *Climate Dyn.*, **16**, 755–774.
- White, W. B., Y. M. Tourre, M. Barlow, and M. Dettinger, 2003: A delayed action oscillator shared by biennial, interannual, and decadal signals in the Pacific Basin. *J. Geophys. Res.*, **108**, 3070, doi:10.1029/2002JC001490.
- Zhang, Y., J. M. Wallace, and D. S. Battisti, 1997: ENSO-like interdecadal variability: 1900–1993. *J. Climate*, **10**, 1004–1020.